Plant Soil (2023) 489:613–628
https://doi.org/10.1007/s11104-023-06047-x

RESEARCH ARTICLE

Mean nutrient uptake depths of cereal crops change with compost incorporation into subsoil – evidence from $^{87}Sr/^{86}Sr$ ratios

David Uhlig · Anne E. Berns · Bei Wu · Wulf Amelung

Received: 14 November 2022 / Accepted: 20 April 2023 / Published online: 8 May 2023

Abstract

Background and Aims Root restricting layers often hinder crops from accessing the large reservoir of bioavailable mineral nutrients situated in subsoil. This study aims to explore changes in the mean nutrient uptake depth of cereal crops when removing root restricting layers through subsoil management.

Methods Subsoil management was performed by deep loosening, cultivation of lucerne as deep-rooting pre-crop, and their combination with compost incorporation. Management effects were evaluated by means of shoot biomass and element concentrations in shoots and soil compartments. The mean nutrient uptake depth was fingerprinted by graphically matching the $^{87}Sr/^{86}Sr$ ratios in shoots with the $^{87}Sr/^{86}Sr$ ratios in the exchangeable fraction in soil. Nutrient uplift from depth to topsoil was inferred from element concentrations in the exchangeable fraction in soil.

Results Shoot biomass remained constant in management and control plots. The mean nutrient uptake depth changed with subsoil management in the order: deep loosening < control < deep loosening with compost incorporation. The latter coincided with a reallocation of compost-derived Na and hence resulted in increased levels of bioavailable Na below the depth of compost incorporation, which may have led to an improved water use efficiency of the crops. Thus, Na relocation triggered the deepening of the mean uptake depth of water and nutrients. Moreover, nutrient uplift from depth to topsoil was evident 21 months after subsoiling.

Conclusion Subsoil management by deep loosening with compost incorporation provides a sustainable use of soil resources because otherwise unused deep geogenic-derived nutrient reservoirs were additionally involved in crop nutrition.

Keyword Nutrient uplift · Sustainable agriculture · Radiogenic Sr · Spring barley · Winter wheat

Responsible Editor: Hans Lambers.

D. Uhlig (✉) · A. E. Berns · B. Wu · W. Amelung
Institute of Bio- and Geosciences (IBG-3) Agrosphere, Forschungszentrum Jülich GmbH, Wilhelm-Johnen-Straße, 52428 Jülich, Germany
e-mail: d.uhlig@fu-berlin.de

Present Address:
D. Uhlig · W. Amelung
Institut für Geologische Wissenschaften, Freie Universität Berlin, - Malteser Str. 74-100, 12249 Berlin, Germany

W. Amelung
Institute of Crop Science and Resource Conservation – Soil Science and Soil Ecology, University of Bonn, Nussallee 13, 53115 Bonn, Germany

Introduction

The global population is rising to about 10 billion people by 2050 (Adam 2021). This population growth dramatically increases human demand for agricultural products. From 1961 to 2017, for example, global

cereal production was boosted by about 240% (IPCC 2019). Negative effects of this development are omnipresent and include land use changes like deforestation, groundwater pollution, and freshwater depletion (Campbell et al. 2017). To avoid further conversions of natural ecosystems into intensely managed agricultural land and to cope with prolonged summer droughts resulting from climate warming, an efficient use of soil resources is urgently required.

Traditionally, the productivity of agricultural land was almost exclusively maintained in the plough horizon, the agricultural topsoil. However, the subsoil beneath this tilled layer contains an inherent large reservoir of water and mineral nutrients in bioavailable form (Kirkegaard et al. 2007; Kautz et al. 2013). Given the global mean maximum rooting depth of crops of 200 cm (Canadell et al. 1996) these resources are principally accessible to crops. However, the most common arable crops have shallower maximum rooting depths ranging from about 50 cm to 150 cm depth (Fan et al. 2016). Thus, projects like DeepFrontier (Thorup-Kristensen et al. 2020) aimed at developing deep rooting crops by breeding (Wasson et al. 2012), or by improving deep rooting through crop management such as early sowing (Rasmussen and Thorup-Kristensen 2016) and crop rotation (Thorup-Kristensen and Kirkegaard 2016). Further suggestions on the exploitation of deep soil layers by crops include a change from annual to perennial crop species (Glover et al. 2010; Crews and Cattani 2018), planting deep rooting pre-crops on arable soil (Perkons et al. 2014; Seidel et al. 2019), and agroforestry, where shallow rooted crops are intercropped with deep rooted species (Cardinael et al. 2015).

However, many soils have root restricting layers in the upper meter of soil, which affect, for example, up to 71% of Germany's agricultural soils (Schneider and Don 2019a). Effective means to reduce the penetration resistance for crops include physical melioration such as deep loosening (Schneider and Don 2019b). Deep loosening enhances not only root growth into the subsoil (Jakobs et al. 2019) but also increases water infiltration (Blanco-Canqui et al. 2017), which promotes crop yield especially in dry years (Marks and Soane 1987; Olesen and Munkholm 2007; Gaiser et al. 2012). Deep loosening combined with the incorporation of compost improves grain yield (Jakobs et al. 2019). Whether deep loosening also results in a deepening of the uptake depth of water and nutrients, and even causes nutrient uplift, remains elusive. Nutrient uplift, as a result of uptake of nutrients from the mineral soil and their return to the organic topsoil via multiple pathways, leaves behind a characteristic depth profile of increasing concentrations of the most plant essential nutrient elements in the exchangeable and extractable fraction of soil from depth to topsoil (Jobbágy and Jackson 2001). Thus, even though nutrient uplift can easily be detected by means of concentration measurements, it remains unknown from which depth uplifted nutrients are originally sourced. Given that root length measurements are highly demanding, an alternative potential analytical tool is a geochemical proxy such as the radiogenic strontium isotope ratio $^{87}Sr/^{86}Sr$.

Strontium has four stable isotopes (^{84}Sr, ^{86}Sr, ^{87}Sr, ^{88}Sr), among which ^{87}Sr results from the radioactive β^- decay of ^{87}Rb (half-life time $= 4.88 \times 10^{10}$ yr^{-1} (Holden 1990)), eponymous for this 'radiogenic' isotope system. Unlike for non-traditional stable isotopes, any natural and instrumental mass-dependent isotope fractionation affecting the $^{87}Sr/^{86}Sr$ ratio is corrected for online during mass spectrometric measurements. Thus, the $^{87}Sr/^{86}Sr$ ratio of primary minerals only depends on its original ratios of $^{87}Rb/^{86}Sr$ and $^{87}Sr/^{86}Sr$, and geological age. Following chemical weathering and biological uptake of Sr, inorganic and organic matter carries the $^{87}Sr/^{86}Sr$ ratio of its source. Comprehensively, the $^{87}Sr/^{86}Sr$ ratio has become the proxy of choice in provenance studies aiming at fingerprinting the geographical origin of terrestrial material across scientific disciplines including anthropology, archaeology, ecology, geochemistry, and geology. For example, in the agricultural sector $^{87}Sr/^{86}Sr$ ratios were applied to trace the origin of beverages such as wine (e.g., Almeida and Vasconcelos 2001; Marchionni et al. 2013; Coldwell et al. 2022), orange juice (Rummel et al. 2010), and bottled water (e.g., Montgomery et al. 2006; Voerkelius et al. 2010); foods such as rice (Kawasaki et al. 2002; Ariyama et al. 2012), wheat (Liu et al. 2016, 2017), olives (Techer et al. 2017), onions (Hiraoka et al. 2016), and other vegetables (e.g., Swoboda et al. 2008; Song et al. 2014; Aoyama et al. 2017); and products with stimulating effects such as coffee beans (Rodrigues et al. 2011) and marijuana (West et al. 2009). Whereas in these studies the $^{87}Sr/^{86}Sr$ ratio of the products is directly matched with the $^{87}Sr/^{86}Sr$ ratio of the source as a whole, the radiogenic Sr isotope ratio is also suited to fingerprint the depth of Sr uptake across an individual soil depth

profile. In doing so, the $^{87}Sr/^{86}Sr$ ratio of individual plant organs pinpoints the $^{87}Sr/^{86}Sr$ ratio of the bioavailable fraction of Sr in soil – that is Sr in soil water and/or the exchangeable fraction of Sr in soil (Song et al. 2014) – as demonstrated for grass, shrubs and trees (McCulley et al. 2004; Poszwa et al. 2004; Bélanger and Holmden 2010; Coble et al. 2015; Aguzzoni et al. 2019; Uhlig et al. 2020).

The objective of this study was to evaluate field experiments in which subsoil management was performed by deep loosening in different ways, and to explore the following questions by means of the elemental composition and the radiogenic Sr isotope ratio of shoots and their soil resources: 1.) To which depth does deep loosening deepen the nutrient uptake depth? 2.) Does deep loosening trigger nutrient uplift? 3.) If so, how fast is nutrient uplift?

Materials and methods

Field site

The field study was conducted at the Experimental Station of the University of Bonn "Campus Klein-Altendorf" located in Rheinbach (6° 59′ 29'' E, 50° 37′ 21'' N). The climate is temperate and humid with a long-term (1956 to 2020) mean annual temperature of 9.6 °C, mean annual precipitation of 603 mm, and a pronounced water deficit of about -640 mm throughout the summer season. The soil is classified as Haplic Luvisol (hypereutric, siltic) developed from loess (IUSS Working Group WRB. 2015), and is characterized by a silty clay loam texture with clay accumulation in the subsoil between 45 and 95 cm soil depth. The $CaCO_3$ content is < 1 g kg^{-1} from 0 – 1.27 m soil depth and rises to 127 g kg^{-1} below 1.27 m depth (Barej et al. 2014). The bulk soil density increases from 1.29 g cm^{-3} to 1.52 g cm^{-3} from topsoil to 1 m soil depth (Barej et al. 2014). For a more detailed description of the soil the reader is referred to Barej et al. (2014).

Experimental field trial and subsoil management

Field experiments were conducted at two central field trials (CF), namely CF 1–1 and CF 2, being ~2.1 km apart from each other. Each central field trial was subdivided into single plots allowing various subsoil management methods complemented by a control with three field replicates at CF 1–1, and four field replicates at CF 2. A detailed description on the technical realization of subsoil management is given in Jakobs et al. (2019), Hinzmann et al. (2021), Schmittmann et al. (2021). In brief, subsoil management was carried out by strip-wise melioration in September of the respective starting year (CF 1–1: 2016, CF 2: 2019) and included i) deep loosening (DL), ii) deep loosening with the incorporation of biowaste compost (DLB) from kitchen waste of private households, and iii) deep loosening with biowaste compost in combination with the deep rooting pre-crop lucerne (DLB luc.). Quantities of incorporated organic material amounted to 5 kg m^{-2} at CF 1–1 and 3 kg m^{-2} at CF 2. Deep loosening was applied to a depth of 60 cm. At CF 1–1 organic material was manually incorporated into subsoil by strip wise removing topsoil, mixing compost with subsoil from the E/B and Bt1 horizon at 30 cm to 60 cm depth and re-adding topsoil. To allow strip wise subsoil management of a larger area, organic material was mechanically incorporated at CF 2 into the E/B horizon ranging from 30 to 45 cm. Visual inspections did not provide indications that there was any unwanted admixture of compost into the Ap horizon during compost incorporation into subsoil. Prior to the subsoil management both central field trials were limed with converter lime (Lhoist Germany, Rheinkalk GmbH) in 2015 (0.3 kg m^{-2}) and 2016 (0.4 kg m^{-2}) and annually fertilized with ~30 g m^{-2} calcium ammonium nitrate. Preceding cultivars were wheat and barley at CF 1–1 and grass at CF 2. In addition, only at CF 2 lucerne was cultivated as pre-crop in 2016 in half of the field plots, regularly harvested, and mulched in 2018. After subsoil management mustard was sown at both field trials as catch crop and mulched prior to performing a crop rotation in the order of spring barley followed by winter wheat. Winter wheat at CF 1–1 was sown on 23rd October 2017 and spring barley at CF 2 was sown on 25th March 2020. No irrigation was performed from sowing to sampling.

Sampling and sample preparation

Winter wheat (*Triticum aestivum L.*) and spring barley (*Hordeum vulgare L.*) were sampled at flowering stage on 30th May 2018 at CF 1–1 and on 22nd June

2020 at CF 2, respectively. In doing so, bunches of aboveground shoots were collected from each field replicate, each of which contained a minimum of ten shoots. The reason for omitting roots from sampling was that only the topmost part of the roots was removable from the hardened topsoil. Thus, root biomass, accounting for about a third of the crop's total biomass under non nutrient deficient conditions (Lopez et al. 2023), would have been sampled incompletely. Representative aliquots of biowaste compost were taken in 2016 at CF 1–1 only.

Soil sampling was performed on the same day of crop sampling beneath the sampled shoot. At CF 1–1 soil samples were collected from soil cores taken with a soil auger of 6 cm inner diameter lined with an inner plastic sleeve for sample recovery. At CF 2 soil samples were taken from freshly excavated soil pits. Composite soil samples of the respective soil horizon were taken to 1 m depth. Specifically, the depth intervals of 0 – 30 cm (Ap horizon), 30 – 50 cm (E/B horizon), 50 – 60 cm (Bt1 horizon), 60 – 70 cm (Bt2 horizon), 70 – 100 cm (Bt3 horizon) were sampled at CF 1–1. At CF 2 the open soil pit allowed for a higher sampling resolution from 0 – 10 cm (Ap horizon), 10 – 20 cm (Ap horizon), 20 – 30 cm (Ap horizon), 30 – 45 cm (E/B horizon), 45 – 60 cm (Bt1 horizon), 60 – 80 cm (Bt2 horizon), 80 – 100 cm (Bt3 horizon). An aliquot of converter lime of a batch from 2021 (Lhoist Germany, Rheinkalk GmbH) was collected because reference samples from 2015–2016 were consumed for previous analyses.

Plant and soil samples were transferred from field to laboratory on the day of sampling and frozen at − 20 °C. Prior to soil sieving (< 2 mm fraction), or dissection of plant samples into whole ear, stem and leaves, samples were dried by lyophilization for a minimum of 24 h at − 55 °C using a Christ Beta 1-8LD plus freeze drier (Martin Christ Gefriertrocknungsanlagen GmbH, Germany). Aliquots of compost and converter lime were dried in an oven for 24 h at 60 °C. Plant organs were milled in 100 ml sealable HDPE bottles equipped with tungsten carbide milling balls using a shaker (Collomix Agia 330, Collomix GmbH, Germany). To minimize analytical effort and costs particularly on the analyses of Sr isotope ratios the field replicates of soil samples were pooled and homogenized using a rotator overhead shaker (BioSan Multi Bio RS-24, Germany).

Analytical methods

Soil digestion using $Li_2B_4O_7$ fusion and the analyses of element concentrations using inductively coupled plasma optical emission spectroscopy (ICP-OES) was performed at the Central Institute of Engineering, Electronics and Analytics (ZEA-3) of Forschungszentrum Jülich GmbH. The remaining analytics comprising microwave assisted sample digestion, element concentration analyses by quadrupole inductively coupled plasma mass spectrometry (ICP-MS), analyses of loss on ignition, and Sr isotope ratios by multi-collector inductively coupled plasma mass spectrometry (MC-ICP-MS) were performed at the Institute of Bio- and Geosciences (IBG-3) at Forschungszentrum Jülich GmbH that is equipped with a self-made, low particulate clean laboratory.

Sample digestion and concentration analyses

Plant and compost samples. A maximum of 400 mg of powdered and homogenized whole ears, stems, leaves, and compost were digested using a pressurized microwave digestion system (turboWAVE, Milestone Srl, Italy) and a mixture comprising 3.5 ml 15 M HNO_3, 2 ml 30% H_2O_2 and 2.5 ml deionized water (18.2 MΩ cm, TOC < 3 ng g^{-1}, Merck Millipore, Germany). Plant digests were centrifuged at 8000 rpm for 5 min (Beckman-Coulter Allegra X30R, USA, with a rotor of fixed-angle (25°) and a maximum radius of 97 mm) to separate the dissolved sample from silicate residues and the supernatant was pipetted off. The residuum was rinsed three times each with 1 ml deionized water, centrifuged and the supernatants were combined to ensure the complete transfer of the dissolved sample. Element concentrations were analysed by ICP-OES (iCAP 6500, Thermo Scientific, Germany) following the Cs-HNO_3 method described in Schuessler et al. (2016). Relative uncertainties, given as the relative deviation of the measured element concentration of a standard reference material (SRM) to its certified value, were assessed by processing NIST SRM 1515 apple leaves with each sample digestion batch and by processing NIST SRM 1573a tomato leaves, NIST SRM 1575a pine needles and ERM-CD281 rye grass occasionally. Relative uncertainties were reported in Table S5 (Uhlig 2022) and typically amounted to better than ± 10%.

Element concentrations of shoots ($[X]_{shoot}$) were calculated from Eq. 1, where j refers to the crop organs ear, stem, or leaf, and f denotes the relative proportion of the dry biomass of the respective crop organ j to the total dry biomass of the shoot.

$$[X]_{shoot} = \sum_{j=organ}^{j} [X]_j \bullet f_j \quad (1)$$

Bulk soil and converter lime samples. Prior to digestion a representative aliquot of 1 g of pooled and homogenized soil was milled using an agate mortar and pestle. Then, fusion digestion was performed by mixing 50 mg of soil with 250 mg of $Li_2B_4O_7$ followed by heating at 1050 °C for 30 min in a muffle furnace. Element concentrations were analysed by ICP-OES (iCAP 6500, Thermo Scientific, Germany) and concentrations of major elements were expressed as oxide concentrations. Loss on ignition (LOI) was determined by heating 0.5 g of soil at 550 °C for 2 h in a muffle furnace to rescale oxide concentrations to 100%. An aliquot of 50 mg of converter lime was dissolved in 6 M HCl, evaporated to dryness and re-dissolved in 0.3 M HNO_3. Element concentrations of converter lime were analysed by ICP-MS (Agilent 7900, Agilent Technologies Inc., USA). Relative uncertainties of the fusion digestion were assessed by repeat digestion of NIST SRM 2709a San Joaquin soil, reported in Table S1b (Uhlig 2022), and typically amounted to better than ± 5%.

Exchangeable fraction in soil

The exchangeable fraction in soil was extracted by suspending two grams of dried and sieved soil (< 2 mm fraction) in 20 ml of 1 M NH_4OAc and gently shaking this suspension for 2 h with a rotator overhead shaker (BioSan Multi Bio RS-24, Germany). The suspension was centrifuged at 8000 rpm for 5 min, and the supernatant was passed through a 0.20 µm acetate filter. Element concentrations were measured by ICP-MS (Agilent 7900, Agilent Technologies Inc., USA). Relative uncertainties were assessed by repeat analyses of NIST SRM 1640a natural water that is appropriate to resemble the sample matrix of the exchangeable fraction in soil, reported in Table S4 (Uhlig 2022), and typically amounted to better than ± 5% (Table S4).

Radiogenic Sr isotopes

Strontium was purified from matrix elements using converted disposable pipettes packed with 200 µl TrisKem SR-B50-S resin (50–100 µm). A sample aliquot containing 400 ng Sr was loaded onto the resin. Matrix elements were removed by elution with 5.5 ml 7.5 M HNO_3 and Sr was eluted with 2 ml deionized water. After evaporation to dryness, organic crown-ethers released from the Sr resin were oxidized in a 1:1 (v/v) mixture comprising 30% H_2O_2 and concentrated HNO_3, heated in closed PFA vials first for 1 h at 85° C and then for 3 h at 170 °C. After evaporation to dryness and redissolution in 0.3 M HNO_3 the purity of the Sr fraction was checked by ICP-MS analysis.

The $^{87}Sr/^{86}Sr$ ratio was measured with a MC-ICP-MS (Nu Plasma II, Nu Instruments Ltd, UK) equipped with an APEX-IR (Elemental Scientific Inc., USA) at low mass resolution in 1 block of 100 cycles with 10 s integration time. The intensity of the blank yielded ≤ 20 mV, which was negligible compared with the intensity of the sample yielding about 20 V on mass 88. The signals of the masses 82, 83 and 85 were measured together with the Sr masses (84, 86, 87, 88) to correct for Kr and Rb interferences on mass 84 and 87, respectively. The measured $^{87}Sr/^{86}Sr$ ratio was normalized to the $^{86}Sr/^{88}Sr$ ratio of 0.1194 (Steiger and Jager 1977) using an exponential law to correct for natural and instrumental mass-dependent isotope fractionation. Repeated analyses of SRM 987 with and without Sr purification were used to determine the long-term accuracy of the method yielding mean values and two standard deviations of 0.71029 ± 0.00004 (N = 6, with Sr purification) and 0.71028 ± 0.00006 (N = 67, without Sr purification). Within two standard deviations the measured $^{87}Sr/^{86}Sr$ ratios of SRM 987 agree with its reference ratio (0.71025 ± 0.00005, level of confidence 95%, N = 474) reported in the GeoReM database (Jochum et al. (2005), http://georem.mpch-mainz.gwdg.de) for MC-ICP-MS analyses.

Statistical analysis

Null hypothesis significance testing was carried out on the difference among the control and subsoil managed plots in the variables i) biomass, ii) element

concentrations and iii) Sr isotope ratios using the data analysis software OriginPro 2022 (version 9.9.0.225; OriginLab Corporation; Northampton, MA, USA). Because field replicates of soil samples were pooled, statistical analyses were limited to field replicates of shoots. Prior to significance testing, datasets were checked for normal distribution (Shapiro–Wilk, $p < 0.05$) and variance equality (two sample F-test, $p < 0.05$). If both apply, the significance of difference was analysed using a two-sample t-test ($p < 0.05$). In case of variance inhomogeneity, a Welch-correction was performed. In case of non-normally distributed datasets, a non-parametric test was performed (Wilcoxon-Mann–Whitney test, $p < 0.05$).

Results

The elemental composition and the radiogenic Sr isotope ratio of individual crop organs, compost, converter lime and pooled soil samples including bulk soil ($Li_2B_4O_7$ digestion) and the exchangeable fraction in soil (1 M NH_4OAc) is reported in Table S1-S5 (Uhlig 2022). Biomass and element concentrations of shoots averaged from individual field replicates are summarized in Table 1. Concentrations of selected elements, namely macronutrients (K, Ca, Mg, P), micronutrients (Fe, Mn, Zn), a plant beneficial element (Na), and non-nutritive elements (Ba, Sr) are displayed for the CF 1–1 trial in Fig. 1 and for the CF 2 trial in Fig. 2 for the compartments shoots (panels: a-e, p–t), the exchangeable fraction in soil (panels: f-j, u-y), and bulk soil (panels: k–o, z-ad). The $^{87}Sr/^{86}Sr$ ratios are shown in Fig. 3 for both trials.

Shoot biomass (Table 1) and bulk soil density (not shown, personal communication, Julien Guigue, September 2022) among control and managed plots were identical within uncertainty. Therefore, element concentrations rather than element stocks were considered hereafter. Overall, element concentrations of shoots, the exchangeable fraction in soil, and bulk soil were identical among control and deep loosening (DL) plots. Consequently, no management effects could be found with DL. In contrast, element concentrations and the radiogenic Sr isotope ratio of mainly the exchangeable fraction in soil differed from the control plots, when DL was combined with the incorporation of biowaste compost (DLB) and when lucerne (luc.) was cultivated as deep rooting pre-crop. Consequently, management effects were found with DLB and DLB luc., which are detailed next.

Elemental composition of shoots and soil compartments

Shoots barely responded to subsoil management with biowaste compost (DLB). Exceptions towards increased element concentrations at DLB plots of both trials were found for the plant-beneficial element Na. Its magnitude was much more pronounced than for micronutrients like Zn at CF 1–1, and Fe and Mn at CF 2. However, pre-cropping with the deep rooting lucerne resulted in an increase in element concentrations of Na, Mn, and P in shoots cultivated on the control plots. Beyond that, concentrations of the macronutrients Ca and Mg (both CF trials) and concentrations of the micronutrients Fe and Mn (CF 2) were lower than required for adequate growth (cf. data points with vertical dashed green lines in Fig. 1 and Fig. 2). Yet, the possibility of growth limitation was discounted because shoot biomass remained identical among the control and DLB plots.

The exchangeable fraction in soil showed management effects at both CF trials. At CF 1–1, concentrations of K, Ca and Na increased at the depth of compost incorporation and above (K, Ca, Mg, P) or below (Na). At CF 2, all elements responded to subsoil management, indicated by increased concentrations of K, Ca, Mg, P, Na, Fe, Mn and Sr, and decreased concentrations of Zn and Ba at the depth of compost incorporation.

Bulk soil revealed management effects towards increased concentrations of Ca, P, Zn, and Sr at the depth of compost incorporation at CF 2. These effects were consistent with the admixture of biowaste compost being three to five times higher in concentration of these elements than bulk soil. The relative contribution of elements in the exchangeable fraction to bulk soil was on average about 31% (Ca), 6.1% (Sr), 4.7% (Ba), 2.6% (Mg), < 1% (remaining elements). Thus, apart from Ca only a minor fraction of mono- and bivalent elements was bioavailable in soil.

Radiogenic strontium isotope ratios

In shoots, the radiogenic strontium isotope ratios ($^{87}Sr/^{86}Sr$) ranged from 0.70974 to 0.71159 and were identical among the individual shoot organs ear, stem, and leaf (Fig. 3g-j). This equality justified the limitation of $^{87}Sr/^{86}Sr$ ratio analyses to ears at the CF 1–1 trial. The

Table 1 Elemental composition of shoots averaged from individual field replicates at central field trials

Treatment	biomass	Macronutrients				Micronutrients				
		K	Ca	Mg	P	Fe	Mn	Zn	Cu	B
	(g)	(µg g^{-1})	(µg g^{-1})	(µg g^{-1})	(µg g^{-1})	(µg g^{-1})	(µg g^{-1})	(µg g^{-1})	(µg g^{-1})	(µg g^{-1})
CF 1–1 (winter wheat at flowering 2018)										
C (mean)	3.5	13,040	1923	662	1859	102	38	12	2.0	2.3
C (SE)	*0.51*	*4697*	*925*	*254*	*698*	*61*	*14*	*4.5*	*0.78*	*0.94*
DL (mean)	3.1	14,467	1917	690	2047	68	36	14	2.3	2.5
DL (SE)	*0.18*	*2140*	*520*	*169*	*330*	*26*	*5.4*	*3.5*	*0.51*	*0.41*
DLB (mean)	3.5	17,109	2196	790	2209	77	31	17	2.4	2.4
DLB (SE)	*0.19*	*5499*	*885*	*242*	*468*	*72*	*11*	*7.6*	*0.61*	*0.53*
CF 2 (spring barley at flowering 2020)										
C (mean)	1.9	12,853	3065	863	2012	37	15	15	3.0	2.7
C (SE)	*0.20*	*2291*	*836*	*130*	*355*	*9.2*	*2.7*	*2.6*	*0.51*	*0.68*
C luc. (mean)	2.1	14,263	3621	881	1622	33	19	17	3.0	2.4
C luc. (SE)	*0.14*	*1743*	*683*	*96*	*204*	*7.1*	*3.0*	*1.9*	*0.34*	*0.36*
DLB (mean)	1.9	12,454	3362	861	1969	38	22	16	2.8	2.4
DLB (SE)	*0.01*	*1106*	*451*	*83*	*239*	*7.4*	*2.3*	*1.6*	*0.27*	*0.23*
DLB luc. (mean)	1.9	13,844	3238	893	1727	42	24	22	3.1	2.4
DLB luc. (SE)	*0.04*	*1014*	*269*	*56*	*118*	*4.3*	*3.7*	*9.3*	*0.20*	*0.19*

	Beneficial elements			Non-nutritive elements				
	Na	Al	Co	Ba	Sr	Ti	Cr	Li
	(µg g^{-1})	(µg g^{-1})	(µg g^{-1})	(µg g^{-1})	(µg g^{-1})	(µg g^{-1})	(ng g^{-1})	(ng g^{-1})
CF 1–1 (winter wheat at flowering 2018)								
C (mean)	59	70	5.9	6.1	4.2	4.1	224	55
C (SE)	*57*	*76*	*4.6*	*2.5*	*1.8*	*1.9*	*120*	*50*
DL (mean)	33	71	4.9	6.8	4.4	3.6	211	57
DL (SE)	*13*	*42*	*1.4*	*1.9*	*0.73*	*2.7*	*75*	*25*
DLB (mean)	203	82	3.9	8.5	4.8	3.3	218	69
DLB (SE)	*103*	*107*	*4.7*	*4.2*	*1.6*	*2.2*	*178*	*76*
CF 2 (spring barley at flowering 2020)								
C (mean)	303	23	26	9.1	5.9	3.5	199	75
C (SE)	*74*	*9.5*	*6.8*	*2.5*	*1.3*	*0.71*	*92*	*17*
C luc. (mean)	399	18	20	7.3	6.3	2.7	128	70
C luc. (SE)	*71*	*7.7*	*2.8*	*1.0*	*1.2*	*0.38*	*22*	*16*
DLB (mean)	798	21	22	9.4	6.5	3.2	196	68
DLB (SE)	*100*	*9.7*	*3.0*	*1.8*	*0.79*	*0.56*	*37*	*11*
DLB luc. (mean)	770	26	20	8.1	6.1	3.3	182	77
DLB luc. (SE)	*147*	*3.1*	*3.3*	*0.83*	*0.52*	*0.27*	*25*	*11*

SE denotes error propagated standard error obtained from the mean of element concentrations and biomass of plant organs from field replicates

C: control; C luc.: control + lucerne; DL: deep loosening; DLB: deep loosening + biowaste compost; DLB luc.: deep loosening + biowaste compost + lucerne

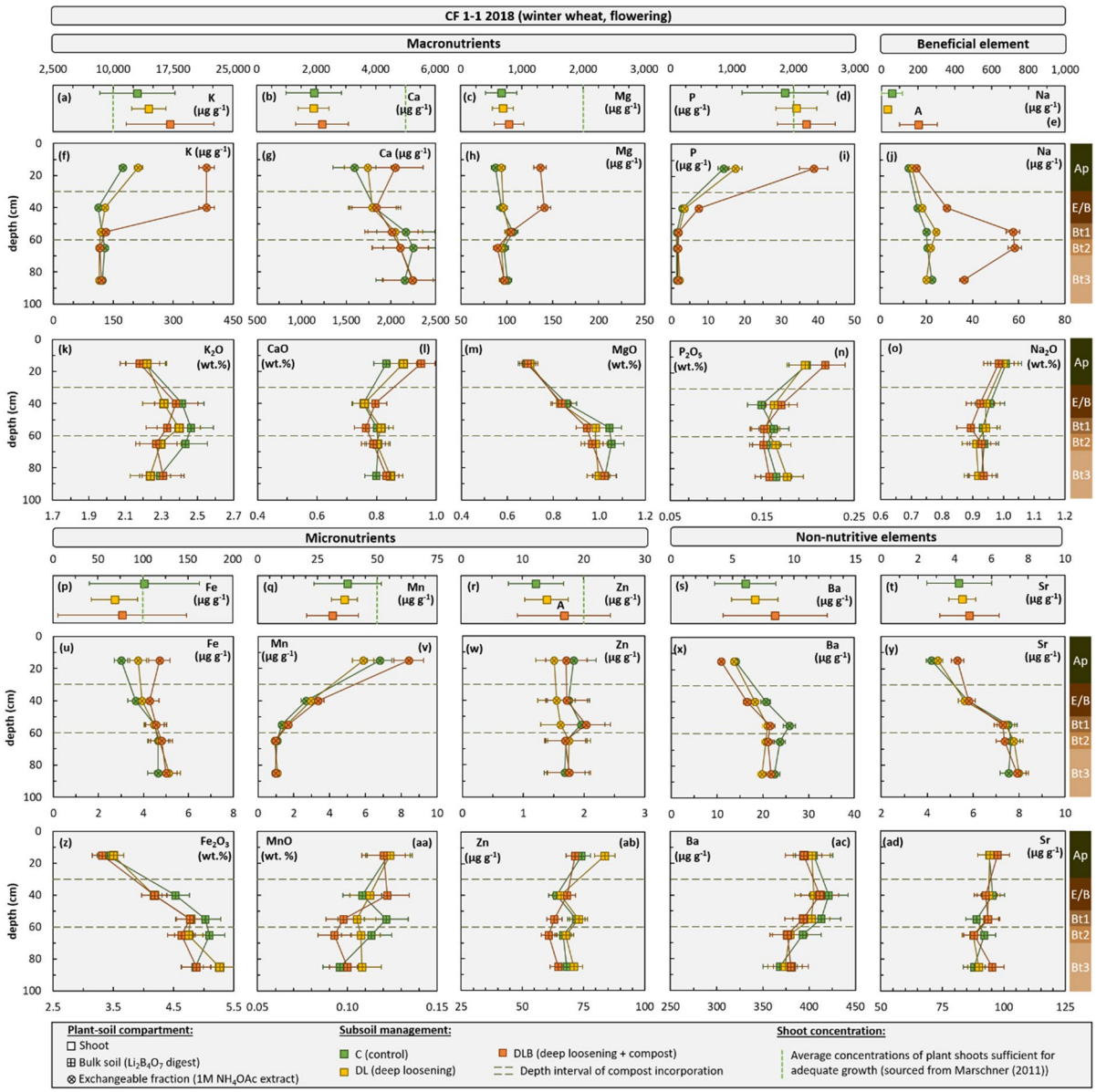

Fig. 1 Selected element concentrations of shoots (panels: (**a**)-(**e**), (**p**)-(**t**)), the exchangeable fraction in soil (panels: (**f**)-(**j**), (**u**)-(**y**)), and element and oxide concentrations in bulk soil (panels: (**k**)-(**o**), (**z**)-(**ad**)) at the central field trial CF 1–1 cultivated with winter wheat under different subsoil managements and the control. Error bars of shoots denote the standard error of field replicates, and error bars of pooled soil samples denote the relative uncertainty reported in Table S1b and Table S3 (Uhlig 2022). Vertical brown bars next to the most right-hand panels illustrate soil horizons according to IUSS Working Group WRB. (2015). Capital letter A indicates significant ($p < 0.05$) concentration differences in shoots among management and the control

$^{87}Sr/^{86}Sr$ ratios of ear replicates at CF 1–1 showed more variation than all shoot organs at CF 2 and were identical among the control and managed plots. In contrast, the $^{87}Sr/^{86}Sr$ ratios of shoot organs significantly differed among the control and managed plots at CF 2.

In the exchangeable fraction, the $^{87}Sr/^{86}Sr$ ratio ranged from 0.70896 to 0.71269 and featured four characteristics. First, $^{87}Sr/^{86}Sr$ increased from topsoil to the base of the sampled subsoil, suggesting the presence of distinct Sr sources in the exchangeable

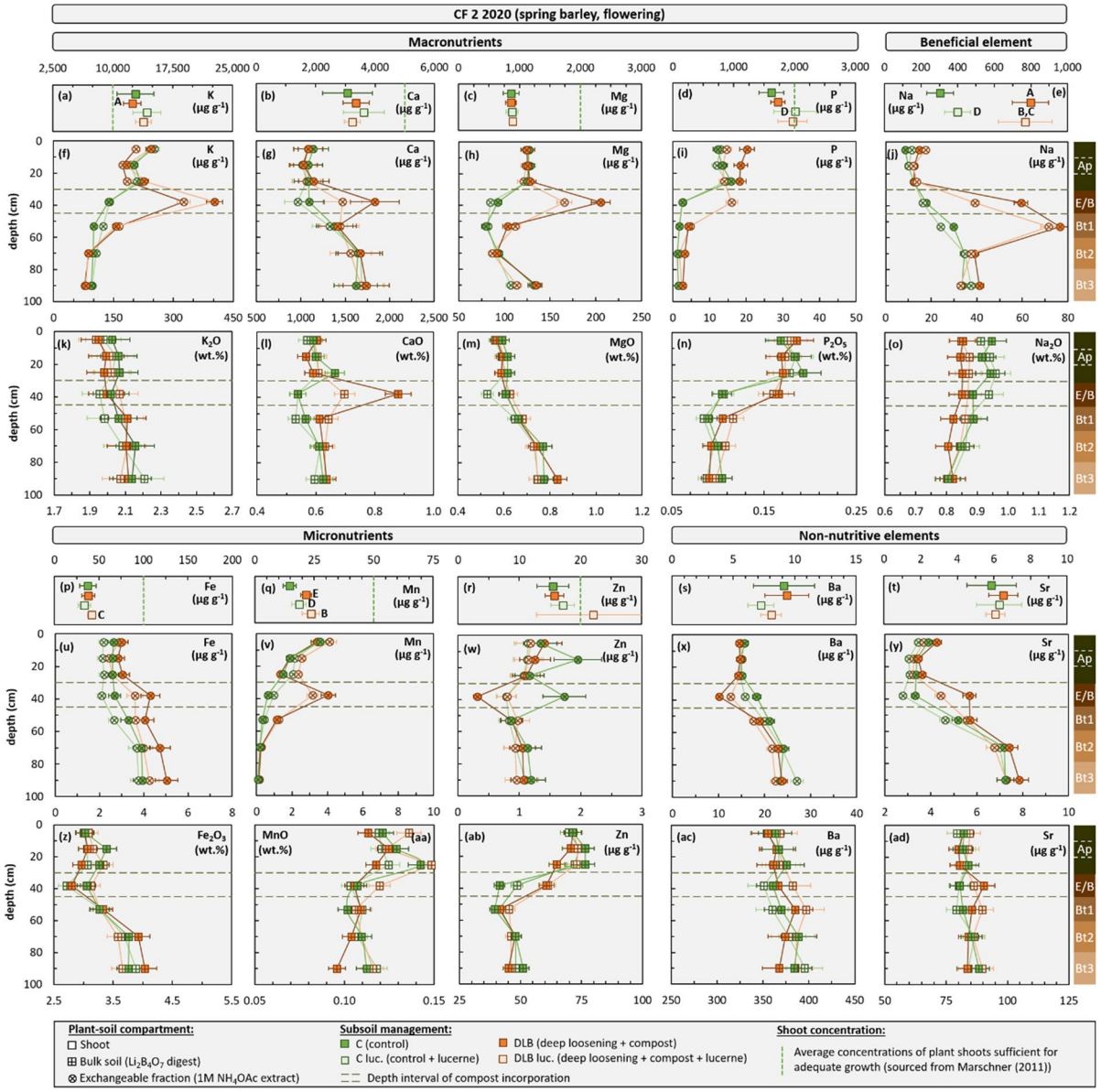

Fig. 2 Selected element concentrations of shoots (panels: (**a**)-(**e**), (**p**)-(**t**)), the exchangeable fraction in soil (panels: (**f**)-(**j**), (**u**)-(**y**)), and element and oxide concentrations in bulk soil (panels: (**k**)-(**o**), (**z**)-(**ad**)) at the central field trial CF 2 cultivated with spring barley under different subsoil managements and the control. Error bars of shoots denote the standard error of field replicates, and error bars of pooled soil samples denote the relative uncertainty reported in Table S1b and Table S3 (Uhlig 2022). Vertical brown bars next to the most right-hand panels illustrate soil horizons according to IUSS Working Group WRB. (2015) and white horizontal dashed lines subdivide the Ap horizon at CF 2 into upper, middle and lower Ap horizon. Capital letters refer to significant ($p < 0.05$) concentration differences in shoots among the control and managed field trial. Specifically, A refers to C – DLB, B refers to C luc. – DLB luc., C refers to C – DLB luc., D refers to C – C luc

fraction with depth. Second, the $^{87}Sr/^{86}Sr$ ratios of all topsoil samples were shifted from more radiogenic $^{87}Sr/^{86}Sr$ ratios towards the less radiogenic $^{87}Sr/^{86}Sr$ ratio of converter lime (0.70913), which is roughly identical with modern-day seawater (0.70918 (Veizer and Compston 1974; Palmer and Edmond 1989; Allègre et al. 2010)). Thus, the dissolution of lime and the subsequent entry of Sr and other elements

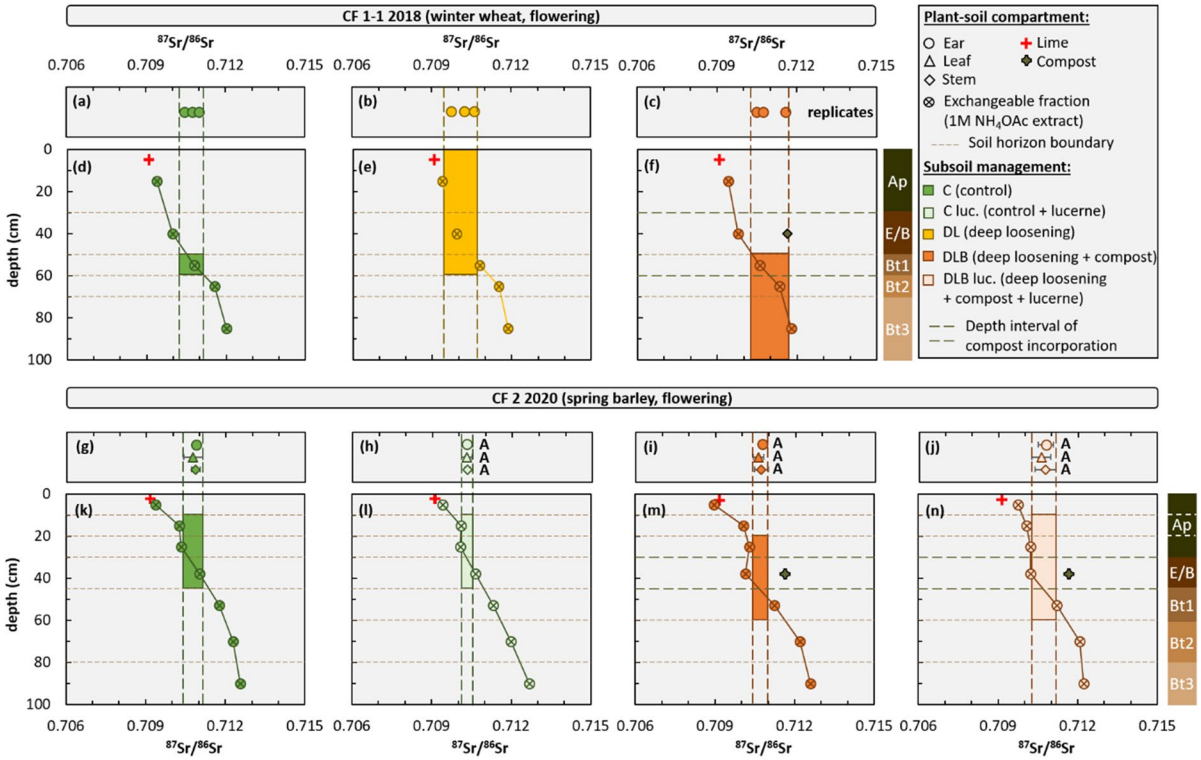

Fig. 3 Radiogenic strontium isotope ratio ($^{87}Sr/^{86}Sr$) of shoots (panels: (**a**)-(**c**), (**g**)-(**j**), Table S5 (Uhlig 2022)) and the exchangeable fraction in soil (panels: (**d**)-(**f**), (**k**)-(**n**), Table S4 (Uhlig 2022)) at the central field trials CF 1–1 (top panels) and CF 2 (bottom panels) cultivated with winter wheat and spring barley under different subsoil managements and the control. Vertical dashed lines bracket the $^{87}Sr/^{86}Sr$ ratios of shoot tissue and filled vertical bars denote a match of the $^{87}Sr/^{86}Sr$ ratio among shoot tissue and the exchangeable fraction in soil in the respective soil horizon. Vertical brown bars next to the most right-hand panels illustrate soil horizons according to (USS Working Group WRB. (2015) and white horizontal dashed lines subdivide the Ap horizon at CF 2 into upper, middle and lower Ap horizon. Error bars of shoots from CF 2 denote the two-fold standard deviation of four field replicates. Error bars of the remaining samples are smaller than the symbol size and refer to the analytical uncertainty (two-fold standard error)

contained in converter lime (e.g., B, Ca, Co, Cu, Cr, Fe, Mg, Mn, Mo, P, Si, Zn) into the exchangeable fraction in soil exerts a major control on the elemental and isotope composition of the exchangeable fraction in topsoil. This finding is consistent with the fact that the application of agricultural lime on non-calcareous soils leads to a change in the elemental and isotope composition of the soil as demonstrated by Thomsen and Andreasen (2019). Third, at CF 2 the $^{87}Sr/^{86}Sr$ ratio was invariant in the lower two Ap horizons, which reflects soil homogenization through ploughing activities throughout past decades. Fourth, consistent with concentration measurements, management effects were evident at CF 2 by two lines of evidence. On the one hand, in both controls the $^{87}Sr/^{86}Sr$ ratios of the exchangeable fraction in the E/B horizon right below the ploughing depth, ranging from 0 – 30 cm, differed from the $^{87}Sr/^{86}Sr$ ratios in the ploughing horizon. On the other hand, the invariance in $^{87}Sr/^{86}Sr$ ratios continued to the E/B horizon at the DLB managed plots. This finding suggests an additional and less radiogenic Sr source in the exchangeable fraction, namely organic-derived Sr, that cannot be found in the bulk digest of biowaste compost. Given that biowaste compost is sourced from multiple kitchen households, Sr is likely present in forms with different solubility. Thus, future studies should additionally focus on the bioavailable form of Sr in compost, which is speculated to be less radiogenic than its bulk digest.

A match of $^{87}Sr/^{86}Sr$ ratios among shoot organs and the exchangeable fraction occurred in different

soil horizons in the control and managed plots. For example, at CF 1–1 an isotope ratio match among ears and the exchangeable fraction occurred in the Bt1 horizon in the control plot, from the Ap to the Bt1 horizon in the DL plot, and from the Bt1 to the Bt3 horizon in the DLB plot. In contrast, at CF 2 an isotope ratio match among shoot organs and the exchangeable fraction occurred from the middle Ap to the E/B horizon in the control and in the control in combination with the deep-rooting pre-crop lucerne. Moreover, an isotope ratio match among crop organs and the exchangeable fraction extended to the Bt1 horizon in the DLB and DLB luc. plots at CF 2.

Discussion

Nutrient uptake depth inferred from $^{87}Sr/^{86}Sr$ ratios

The $^{87}Sr/^{86}Sr$ ratio of crop organs serves as a fingerprint of the $^{87}Sr/^{86}Sr$ ratio of the exchangeable fraction in soil at the depth of Sr uptake. This depth is interpreted as the mean depth from which water and nutritive elements in bioavailable form are sourced. It also encompasses water and nutrient uptake from above this depth, for example, after germination during the crop's early growing stages, and below this depth, for example, at the time of sampling at which the present-day uptake depth is not yet well recorded in the $^{87}Sr/^{86}Sr$ ratio of shoots due to reservoir effects. Four major implications can be drawn from the results.

First, in the control plots the mean nutrient uptake depth of winter wheat lay in the Bt1 horizon, thus ranged from 50 to 60 cm depth (Fig. 3a), whereas the mean nutrient uptake depth of spring barley ranged from the top of the middle Ap horizon at 20 cm depth to the bottom of the E/B horizon at 40 cm depth (Fig. 3k). Consequently, winter wheat took up water and nutrients from greater depth than spring barley. This finding is consistent with the fact that winter wheat spent five months longer on the field upon the day of sampling than spring barley, allowing its roots to reach deeper soil regions than spring barley. According to Thorup-Kristensen et al. (2009) a cultivation sowed in winter (e.g., winter wheat) indeed grows two times deeper into the soil than a cultivation sowed in spring (e.g., spring wheat).

Second, subsoiling by deep loosening alone resulted into a mean nutrient uptake depth, which involved shallower soil horizons than in the control. Specifically, the mean nutrient uptake depth in the DL plots ranged from the topmost Ap horizon at 0 cm depth down to the bottom of the Bt1 horizon at 60 cm depth (Fig. 3b). In contrast, the mean nutrient uptake depth in the control was limited to the Bt1 horizon, thus ranged from 50 to 60 cm depth (Fig. 3a). This finding was surprising because deep loosening was supposed to reduce soil penetration resistance to crop roots to enable roots for the access of deeper soil horizons for crop nutrition than in the non-loosened control. Thus, because deep loosening did not cause a shift of the mean nutrient uptake depth towards deeper soil horizons than in the control, root restricting layers apparently do not occur in the Luvisol at CF 1–1. Instead, deep loosening had the opposite of the supposed effect, namely an intensification of nutrient uptake in shallower soil horizons than in the control, which even hindered roots from foraging into deeper non-loosened soil for water and nutrient uptake.

Third, cultivating lucerne as deep rooting pre-crop resulted in the same mean nutrient uptake depth of the succeeding crops than without pre-cropping with lucerne, which ranged from the top of the middle Ap horizon at 20 cm depth down to the bottom of the E/B horizon at 45 cm depth (Fig. 3l). On the one hand, this finding conflicts with the underlying hypothesis that lucerne creates deep biopores (Han et al. 2015), which allow roots of succeeding crops to develop a deeper rooting system (Han et al. 2017) than without pre-cropping with lucerne. On the other hand, this finding demonstrates that, although lucerne can significantly dry out the subsoil by transpiration, pre-cropping with lucerne had no negative effect on the mean nutrient uptake depth, even when the re-wetting period faces a severe drought with a water deficit amounting to about –640 mm.

Fourth, deep loosening in combination with the incorporation of biowaste compost into subsoil resulted not only in a deepening of the maximum rooting depth (Bauke et al., n.d.) but also in a deepening of the mean nutrient uptake depth (Fig. 3f, m–n), which extended to below the depth of compost incorporation (Fig. 3f, m–n). This deepening can likely be attributed to an improved water holding capacity of the organic matter added to subsoil incorporated into subsoil (Lal 2020).

Shifts in the mean nutrient uptake depth towards deeper soil horizons through DLB and DLB luc. were

also accompanied by increases in element concentrations in shoots. The most affected elements were the redox-sensitive micronutrients Mn (DLB and DLB luc. t CF 2) and Fe (DLB luc. at CF 2), and the plant beneficial element Na (DLB at both trials, and DLB luc. at CF 2). The release of Mn and Fe might have been promoted by increased microbial utilization of the compost substrate, and thus lower redox potential in addition to possible releases of chelating agents. In contrast, the concentration increases of Na cannot solely be attributed to increased abiotic weathering because the soil pH at CF 2 increased from 6.9 in the control plot to 7.5 after compost incorporation into subsoil (Uhlig 2022). Even though some minor portions of nutrients might have been mobilized from subsoil by enhanced chemical weathering caused by microbial priming (Fang et al. 2023), this contribution is likely negligibly small compared with the supply of these elements in bioavailable form with biowaste compost. We thus attributed the increased element concentrations in shoots to peaks in the depth of compost incorporation (DLB and DLB luc. plots). This raises the question, whether subsoiling with compost results not only in nutrient uptake followed by harvest, but also in nutrient uplift, hence in the entry of these elements into the exchangeable and extractable fraction in topsoil as recently speculated by means of Mg stable isotopes at the same field site (Uhlig et al. 2022). A manifestation of which presents a sustainable side-effect of subsoiling with biowaste compost because the large geogenic reservoir of bioavailable nutrients situated below the depth of compost incorporation becomes an active component of the nutrient cycle in the soil–plant system that would otherwise remain unused by plants.

Nutrient uplift

The 'nutrient uplift hypothesis' from Jobbágy and Jackson (2001), formerly known as the 'base pump' (Vejre and Hoppe 1998), implies that mineral nutrients are taken up from the mineral soil, cycled through biota, returned via three potential pathways to topsoil to finally end up in the exchangeable and extractable fraction in topsoil. The three potential pathways include i) throughfall; ii) solubilised litterfall, harvest residues, and necrotic biomass; and iii) the so-called sink-regulated transport that is long-distance transport of nutrients through the phloem and its extrusion by roots back into soil, which is most pronounced for the phloem-mobile macronutrients K, Mg and P (White 2012) and which serves plants for biosensing nutrient availability in the growth medium (Ho and Tsay 2010; Krouk et al. 2010). No matter which pathway applies, soil profiles, strongly affected by nutrient uplift, are characterized by declining concentrations of mineral nutrients in the exchangeable and extractable fraction with depth. The magnitude of this decline is most pronounced for mineral nutrients that often limit plant growth like K and P because a high demand in plants is opposed to a low supply in bioavailable form in the soil (e.g., in the exchangeable and extractable fraction). The timescale over which nutrient uplift occurs was found hitherto to range from years ($\leq$3 yr) after cultivating deep rooting precrops in cropping systems (Han et al. 2021) to more than a decade ($\leq$15 yr) after afforesting a sand dune (Jobbágy and Jackson 2004). However, the depth from which nutrient uplift occurs and the kinetics of nutrient uplift in cropping systems remain poorly constrained. Hence, Han et al. (2021) suggested the performance of tracer experiments to better constrain nutrient uplift in cropping systems. Given that the incorporation of biowaste compost into subsoil added nutrients in bioavailable form to the subsoil (cf. peaking concentrations in the exchangeable fraction at the depth of compost incorporation in Fig. 1f, h, j, Fig. 2f-h) the subsoil experiment performed in the present study can be considered as such a tracer experiment that operates at nutrient concentrations at natural abundance levels. It also circumvents the disadvantage that the $^{87}Sr/^{86}Sr$ ratio is unsuited to trace nutrient return to topsoil in the present study because the $^{87}Sr/^{86}Sr$ ratio in the exchangeable fraction of topsoil is dominated by converter-lime-derived Sr.

Along these lines, nutrient uplift was only found at CF 1–1. The magnitude of nutrient uplift, defined here as the proportional concentration increase in the exchangeable fraction in topsoil from C to DLB plots, was most pronounced for the macronutrients P (175%), K (120%), Mg (55%), and the micronutrient Mn (25%). Thus, the exchangeable fraction in topsoil indeed features a biological imprint, or in other words ecological stoichiometry. Provided that crop nutrition occurred under nutrient sufficient conditions, this form of biological pumping also explains the lack of increased concentrations of K, Mg, P, and Mn (only at CF 1–1) in shoots at the DLB plots.

However, nutrient uplift was not evident at CF 2. The most likely reason is the six-months shorter cultivation period of crops at CF 2 because, in contrast to CF 1–1, winter wheat is not yet integrated into the crop rotation at CF 2. Thus, the interaction time of crops with the soil was longer at CF 1–1 allowing pathway iii) for causing nutrient uplift. Overall, nutrient uplift was evident as early as 21 months after subsoiling with biowaste compost at CF 1–1.

Role of Na in shifting the nutrient uptake depth below the depth of compost incorporation

Although Na showed the most striking management effects towards increased concentrations in shoots and in the exchangeable fraction at the depth of compost incorporation, an uplift of Na into the exchangeable fraction of topsoil was not evident. Instead, Na concentrations peaked in the exchangeable fraction in the soil horizon below the depth of compost incorporation at both CF trials. This concentration peak is attributed to the solubilisation of compost-derived Na followed by its downward movement by gravitational water flow and adsorption at deeper soil horizons. Sodium, as a chemical twin of K in plants (Benito et al. 2014) can replace K (e.g., Subbarao et al. 2003; Wakeel et al. 2010) to act as an additional osmoticum to regulate the movement of stomata, which was found to be faster when Na was involved (Wakeel et al. 2011). Thus, Na reallocated towards deeper soil horizons could have been traced by roots biosensing for nutrient availability and mined to improve the water use efficiency of crops, thereby to cope with the water deficient years that the CF trials experienced. Hence, reallocated Na may have triggered the deepening of the mean nutrient uptake depth to below the depth of compost incorporation. Consequently, subsoiling with compost incorporation may not only improve the water use efficiency of crops but also shift the mean uptake depth of nutrients situated beyond the depth of compost incorporation as shown by means of $^{87}Sr/^{86}Sr$ ratios.

Conclusions

The performance of subsoil management by deep loosening or using lucerne as deep rooting pre-crop, and both of which in combination with compost incorporation was evaluated with respect to the nutrient budget in shoots, the exchangeable fraction in soil and in bulk soil, and the nutrient uptake depth by means of the elemental composition and the radiogenic Sr isotope ratio ($^{87}Sr/^{86}Sr$). Regardless of the applied subsoil management practice, negative effects on the nutrient budget in shoots and soil could not be found. On the contrary, Na contents in shoots consistently increased when subsoiling included compost incorporation. Moreover, using the $^{87}Sr/^{86}Sr$ ratio as a proxy for fingerprinting the mean nutrient uptake depth of crops revealed two key findings. First, subsoiling by deep loosening alone resulted into a more intense involvement of shallower soil horizons in nutrient uptake than in the control. Second, deep loosening with compost incorporation resulted into a deepening of the mean nutrient uptake depth below the depth of compost incorporation. This deepening could be triggered by biosensing roots, which not only traced increased levels of bioavailable Na below the depth of compost incorporation, but also utilized this compost-derived Na to improve the water use efficiency of crops during a summer drought. Finally, in settings, where agricultural lime is applied, the $^{87}Sr/^{86}Sr$ ratio is unsuited to trace nutrient uplift. However, an assessment of the elemental composition of the exchangeable fraction suggested nutrient uplift to occur within 21 months after subsoiling from the depth of compost incorporation into topsoil. Overall, subsoil management by deep loosening with compost incorporation causes a deepening of the mean nutrient uptake depth and nutrient uplift from depth to topsoil, thereby serves to be a more promising soil management practice to utilize soil resources beyond the hitherto intensively managed topsoil in the future.

Acknowledgements The authors are grateful to the German Federal Ministry of Education and Research (BMBF) for funding the project "BonaRes (Module A): Sustainable Subsoil Management—Soil^3-II; subproject C" (grant number 031B0515C), and to the staff of the Campus Klein Altendorf, particularly to Oliver Schmittmann (University of Bonn), for installing the central field experiments. Wulf Amelung also acknowledges support from the Deutsche Forschungsgemeinschaft under Germany's Excellence Strategy, EXC-2070–390732324–PhenoRob. For analytical support, the authors are thankful to Volker Nischwitz, Nadine Wettengl, Sabrina Tückhardt and Ulrike Seeling from the Central Institute of Engineering, Electronics and Analytics (ZEA-3) at Forschungszentrum Jülich GmbH. The authors also acknowledge analytical support from the trainees Anna-Lena Lohe, Antonio Voss, Jan-Philipp Treitz and the student assistants Claudia Tahiraj, Melisande Pfennig, and Ying Xing. Finally, the authors acknowledge Sara R. Kimmig, Roland Bol and two anonymous reviewers for reviewing this manuscript.

Author contribution All authors contributed to the study conception and design. Material preparation, data collection and analysis were performed by David Uhlig. The first draft of the manuscript was written by David Uhlig and all authors commented on previous versions of the manuscript. All authors read and approved the final manuscript.

Funding Open Access funding enabled and organized by Projekt DEAL. This work was supported by the German Federal Ministry of Education and Research (BMBF) for funding the project "BonaRes (Module A): Sustainable Subsoil Management—Soil3-II; subproject C" (grant number 031B0515C).

Data availability Research Data associated with this article can be accessed at GFZ Data Services under the reference Uhlig (2022). Tables S1–S5 include the dataset discussed in this publication along with further background data.

Declarations

Competing interest The authors declare that they have no conflict of interest.

References

Adam D (2021) How Far Will Global Population Rise? Nature 597:462–465

Aguzzoni A, Bassi M, Robatscher P et al (2019) Intra- And inter-tree variability of the 87Sr/86Sr ratio in apple orchards and its correlation with the soil 87Sr/86Sr ratio. J Agric Food Chem 67:5728–5735. https://doi.org/10.1021/acs.jafc.9b01082

Allègre CJ, Louvat P, Gaillardet J et al (2010) The fundamental role of island arc weathering in the oceanic Sr isotope budget. Earth Planet Sci Lett 292:51–56. https://doi.org/10.1016/j.epsl.2010.01.019

Almeida CM, Vasconcelos MTSD (2001) ICP-MS determination of strontium isotope ratio in wine in order to be used as a fingerprint of its regional origin. J Anal at Spectrom 16:607–611. https://doi.org/10.1039/b100307k

Aoyama K, Nakano T, Shin KC (2017) Variation of strontium stable isotope ratios and origins of strontium in Japanese vegetables and comparison with Chinese vegetables. Food Chem 237:1186–1195. https://doi.org/10.1016/j.foodchem.2017.06.027

Ariyama K, Shinozaki M, Kawasaki A (2012) Determination of the geographic origin of rice by chemometrics with strontium and lead isotope ratios and multielement concentrations. J Agric Food Chem 60:1628–1634. https://doi.org/10.1021/jf204296p

Barej JAM, Pätzold S, Perkons U, Amelung W (2014) Phosphorus fractions in bulk subsoil and its biopore systems. Eur J Soil Sci 65:553–561. https://doi.org/10.1111/ejss.12124

Bauke SL, Seidel SJ, Athmann M, Berns AE, Braun M, Gocke MI, Guigue J, Kautz T, Kögel-Knabner I, Ohan J, Rillig MC, Schloter M, Schmittmann O, Schulz S, Uhlig D, Schnepf A, Amelung W (n.d.) Sustainable subsoil management: strip-wise loosening and incorporation of organic material enhances crop performance

Bélanger N, Holmden C (2010) Influence of landscape on the apportionment of Ca nutrition in a Boreal Shield forest of Saskatchewan (Canada) using 87Sr/ 86Sr as a tracer. Can J Soil Sci 90:267–288. https://doi.org/10.4141/cjss09079

Benito B, Haro R, Amtmann A et al (2014) The twins K+ and Na+ in plants. J Plant Physiol 171:723–731. https://doi.org/10.1016/j.jplph.2013.10.014

Blanco-Canqui H, Wienhold BJ, Jin VL et al (2017) Long-term tillage impact on soil hydraulic properties. Soil Tillage Res 170:38–42. https://doi.org/10.1016/j.still.2017.03.001

Campbell BM, Beare DJ, Bennett EM, et al (2017) Agriculture production as a major driver of the earth system exceeding planetary boundaries. Ecol Soc 22(4):8. https://doi.org/10.5751/ES-09595-220408

Canadell J, Jackson RB, Ehleringer JB et al (1996) Maximum rooting depth of vegetation types at the global scale. Oecologia 108:583–595. https://doi.org/10.1007/BF00329030

Cardinael R, Mao Z, Prieto I et al (2015) Competition with winter crops induces deeper rooting of walnut trees in a Mediterranean alley cropping agroforestry system. Plant Soil 391:219–235. https://doi.org/10.1007/s11104-015-2422-8

Coble AA, Hart SC, Ketterer ME et al (2015) Strontium source and depth of uptake shifts with substrate age in semiarid ecosystems. J Geophys Res Biogeosci 120:1069–1077. https://doi.org/10.1002/2015JG002992.Received

Coldwell BC, Pérez NM, Vaca MC et al (2022) Strontium Isotope Systematics of Tenerife Wines (Canary Islands): Tracing Provenance in Ocean Island Terroir. Beverages 8:1–19. https://doi.org/10.3390/beverages8010009

Crews TE, Cattani DJ (2018) Strategies, advances, and challenges in breeding perennial grain crops. SustaiN (switzerland) 10:1–7. https://doi.org/10.3390/su10072192

Fan J, McConkey B, Wang H, Janzen H (2016) Root distribution by depth for temperate agricultural crops. Field Crops Res 189:68–74. https://doi.org/10.1016/j.fcr.2016.02.013

Fang Q, Lu A, Hong H et al (2023) Mineral weathering is linked to microbial priming in the critical zone. Nat Commun 14:1–14. https://doi.org/10.1038/s41467-022-35671-x

Gaiser T, Perkons U, Küpper PM et al (2012) Evidence of improved water uptake from subsoil by spring wheat following lucerne in a temperate humid climate. Field Crops Res 126:56–62. https://doi.org/10.1016/j.fcr.2011.09.019

Glover JD, Reganold JP, Bell LW et al (2010) Increased Food and Ecosystem Security via Perennial Grains. Science 328:1938–1939

Han E, Kautz T, Perkons U et al (2015) Quantification of soil biopore density after perennial fodder cropping. Plant Soil 394:73–85. https://doi.org/10.1007/s11104-015-2488-3

Han E, Kautz T, Huang N, Köpke U (2017) Dynamics of plant nutrient uptake as affected by biopore-associated root growth in arable subsoil. Plant Soil 415:145–160. https://doi.org/10.1007/s11104-016-3150-4

Han E, Li F, Perkons U et al (2021) Can precrops uplift subsoil nutrients to topsoil? Plant Soil 463:329–345. https://doi.org/10.1007/s11104-021-04910-3

Hinzmann M, Ittner S, Kiresiewa Z, Gerdes H (2021) An Acceptance Analysis of Subsoil Amelioration Amongst Agricultural Actors in Two Regions in Germany. Front Agron 3:1–14. https://doi.org/10.3389/fagro.2021.660593

Hiraoka H, Morita S, Izawa A et al (2016) Tracing the geographical origin of onions by strontium isotope ratio and strontium content. Anal Sci 32:781–788. https://doi.org/10.2116/analsci.32.781

Ho CH, Tsay YF (2010) Nitrate, ammonium, and potassium sensing and signaling. Curr Opin Plant Biol 13:604–610. https://doi.org/10.1016/j.pbi.2010.08.005

Holden NE (1990) Total half-lives for selected nuclides. Int Union Pure Appl Chem 62:941–958. https://doi.org/10.1351/pac199062050941

IPCC (2019) Summary for Policymakers. In: Shukla PR, Skea J, Buendia EC, et al. (eds) Climate Change and Land: an IPCC special report on climate change, desertification, land degradation, sustainable land management, food security, and greenhouse gas fluxes in terrestrial ecosystems 1–41

IUSS Working Group WRB (2015) World reference base for soil resources 2014, update 2015, International soil classification system for naming soils and creating legends for soil maps. World Soil Resources Report 106. Rome, Italy: Food and Agriculture Organization of the United Nations

Jakobs I, Schmittmann O, Athmann M et al (2019) Cereal Response to Deep Tillage and Incorporated Organic Fertilizer. Agronomy 9:1–16. https://doi.org/10.3390/agronomy9060296

Jobbágy EG, Jackson RB (2001) The distribution of soil nutrients with depth: Global patterns and the imprint of plants. Biogeochemistry 53:51–77. https://doi.org/10.1023/A:1010760720215

Jobbágy EG, Jackson RB (2004) The uplift of soil nutrients by plants: Biogeochemical consequences across scales. Ecology 85:2380–2389. https://doi.org/10.1890/03-0245

Jochum KP, Nohl U, Herwig K et al (2005) GeoReM: A New Geochemical Database for Reference Materials and Isotopic Standards. Geostand Geoanal Res 29:333–338. https://doi.org/10.1111/j.1751-908X.2005.tb00904.x

Kautz T, Amelung W, Ewert F et al (2013) Nutrient acquisition from arable subsoils in temperate climates: A review. Soil Biol Biochem 57:1003–1022

Kawasaki A, Oda H, Hirata T (2002) Determination of strontium isotope ratio of brown rice for estimating its provenance. Soil Sci Plant Nutr 48:635–640. https://doi.org/10.1080/00380768.2002.10409251

Kirkegaard JA, Lilley JM, Howe GN, Graham JM (2007) Impact of subsoil water use on wheat yield. Aust J Agric Res 58:303–315. https://doi.org/10.1071/AR06285

Krouk G, Lacombe B, Bielach A et al (2010) Nitrate-regulated auxin transport by NRT1.1 defines a mechanism for nutrient sensing in plants. Dev Cell 18:927–937. https://doi.org/10.1016/j.devcel.2010.05.008

Lal R (2020) Soil organic matter and water retention. Agron J 112:3265–3277. https://doi.org/10.1002/agj2.20282

Liu H, Wei Y, Lu H et al (2016) Combination of the 87Sr/86Sr ratio and light stable isotopic values (δ13C, δ15N and δd) for identifying the geographical origin of winter wheat in China. Food Chem 212:367–373. https://doi.org/10.1016/j.foodchem.2016.06.002

Liu H, Wei Y, Lu H et al (2017) The determination and application of 87Sr/86Sr ratio in verifying geographical origin of wheat. J Mass Spectrom 52:248–253. https://doi.org/10.1002/jms.3930

Lopez G, Ahmadi SH, Amelung W, et al (2023) Nutrient deficiency effects on root architecture and root-to- shoot ratio in arable crops. Front Plant Sci 13:1–18. https://doi.org/10.3389/fpls.2022.1067498

Marchionni S, Braschi E, Tommasini S et al (2013) High-precision 87Sr/86Sr analyses in wines and their use as a geological fingerprint for tracing geographic provenance. J Agric Food Chem 61:6822–6831. https://doi.org/10.1021/jf4012592

Marks MJ, Soane GC (1987) Crop and soil response to subsoil loosening, deep incorporation of phosphorus and potassium fertilizer and subsequent soil management on a range of soil types. Part 1: Response of arable crops. Soil Use Manag 3:115–123

McCulley RL, Jobbágy EG, Pockman WT, Jackson RB (2004) Nutrient uptake as a contributing explanation for deep rooting in arid and semi-arid ecosystems. Oecologia 141:620–628. https://doi.org/10.1007/s00442-004-1687-z

Marschner H (2011) Marschner's mineral nutrition of higher plants, academic press, available at: https://www.elsevier.com/books/marschners-mineral-nutrition-of-higher-plants/marschner/978-0-12-384905-2. Accessed 29 Mar 2023

Montgomery J, Evans JA, Wildman G (2006) 87Sr/86Sr isotope composition of bottled British mineral waters for environmental and forensic purposes. Appl Geochem 21:1626–1634. https://doi.org/10.1016/j.apgeochem.2006.07.002

Olesen JE, Munkholm LJ (2007) Subsoil loosening in a crop rotation for organic farming eliminated plough pan with mixed effects on crop yield. Soil Tillage Res 94:376–385. https://doi.org/10.1016/j.still.2006.08.015

OriginPro (2022) https://www.originlab.com/index.aspx?go=Company&pid=1130

Palmer MR, Edmond JM (1989) The strontium isotope budget of the modern ocean. Earth Planet Sci Lett 92:11–26

Perkons U, Kautz T, Köpke U (2014) Root growth response of spring wheat (Triticum aestivum L.) and mallow (Malva sylvestris L.) to biopore generating precrops. In: Proceedings of the 4th ISOFAR Scientific Conference. Building Organic Bridges', at the Organic World Congress 2014, 13–15 Oct., Istanbul, Turkey 477–480

Poszwa A, Ferry B, Dambrine E et al (2004) Variations of bioavailable Sr concentration and 87Sr/86Sr ratio in boreal forest ecosystems. Biogeochemistry 67:1–20

Rasmussen IS, Thorup-Kristensen K (2016) Does earlier sowing of winter wheat improve root growth and N uptake? Field Crops Res 196:10–21. https://doi.org/10.1016/j.fcr.2016.05.009

Rodrigues C, Brunner M, Steiman S et al (2011) Isotopes as tracers of the Hawaiian coffee-producing regions. J Agric Food Chem 59:10239–10246. https://doi.org/10.1021/jf200788p

Rummel S, Hoelzl S, Horn P et al (2010) The combination of stable isotope abundance ratios of H, C, N and S with 87Sr/86Sr for geographical origin assignment of orange juices. Food Chem 118:890–900. https://doi.org/10.1016/j.foodchem.2008.05.115

Schmittmann O, Christ A, Lammers PS (2021) Subsoil melioration with organic material—principle, technology and yield effects. Agronomy 11:1970. https://doi.org/10.3390/agronomy11101970

Schneider F, Don A (2019a) Root-restricting layers in German agricultural soils. Part I: extent and cause. Plant Soil 442:433–451. https://doi.org/10.1007/s11104-019-04185-9

Schneider F, Don A (2019b) Root-restricting layers in German agricultural soils. Part II: Adaptation and melioration strategies. Plant Soil 442:419–432. https://doi.org/10.1007/s11104-019-04185-9

Schuessler JA, Kämpf H, Koch U, Alawi M (2016) Earthquake impact on iron isotope signatures recorded in mineral spring water Suppl. J Geophys Res Solid Earth 121:8548–8568. https://doi.org/10.1002/2016JB013408

Seidel SJ, Gaiser T, Kautz T et al (2019) Estimation of the impact of precrops and climate variability on soil depth-differentiated spring wheat growth and water, nitrogen and phosphorus uptake. Soil Tillage Res 195:104427. https://doi.org/10.1016/j.still.2019.104427

Song BY, Ryu JS, Shin HS, Lee KS (2014) Determination of the source of bioavailable Sr using 87Sr/86Sr tracers: A case study of hot pepper and rice. J Agric Food Chem 62:9232–9238. https://doi.org/10.1021/jf503498r

Steiger RH, Jager E (1977) Convention on the use of decay constants in geo- and cosmochronology. Earth Planet Sctence Lett 36:1977

Subbarao GV, Ito O, Berry WL, Wheeler RM (2003) Sodium - A Functional Plant Nutrient. CRC Crit Rev Plant Sci 22:391–416. https://doi.org/10.1080/07352680390243495

Swoboda S, Brunner M, Boulyga SF et al (2008) Identification of Marchfeld asparagus using Sr isotope ratio measurements by MC-ICP-MS. Anal Bioanal Chem 390:487–494. https://doi.org/10.1007/s00216-007-1582-7

Techer I, Medini S, Janin M, Arregui M (2017) Impact of agricultural practice on the Sr isotopic composition of food products: Application to discriminate the geographic origin of olives and olive oil. Appl Geochem 82:1–14. https://doi.org/10.1016/j.apgeochem.2017.05.010

Thomsen E, Andreasen R (2019) Agricultural lime disturbs natural strontium isotope variations: Implications for provenance and migration studies. Sci Adv 5:1–12. https://doi.org/10.1126/sciadv.aav8083

Thorup-Kristensen K, Kirkegaard J (2016) Root system-based limits to agricultural productivity and efficiency: The farming systems context. Ann Bot 118:573–592. https://doi.org/10.1093/aob/mcw122

Thorup-Kristensen K, Cortasa MS, Loges R (2009) Winter wheat roots grow twice as deep as spring wheat roots, is this important for N uptake and N leaching losses? Plant Soil 322:101–114. https://doi.org/10.1007/s11104-009-9898-z

Thorup-Kristensen K, Halberg N, Nicolaisen M et al (2020) Digging Deeper for Agricultural Resources, the Value of Deep Rooting. Trends Plant Sci 25:406–417. https://doi.org/10.1016/j.tplants.2019.12.007

Uhlig D (2022) Isotope geochemical dataset on subsoil management experiments at Campus Klein-Altendorf. GFZ Data Serv. https://doi.org/10.5880/fidgeo.2022.003

Uhlig D, Amelung W, Von Blanckenburg F (2020) Mineral Nutrients Sourced in Deep Regolith Sustain Long-Term Nutrition of Mountainous Temperate Forest Ecosystems. Global Biogeochem Cycles 34:1–21. https://doi.org/10.1029/2019GB006513

Uhlig D, Wu B, Berns AE, Amelung W (2022) Magnesium stable isotopes as a potential geochemical tool in agronomy – Constraints and opportunities. Chem Geol 611. https://doi.org/10.1016/j.chemgeo.2022.121114

Veizer J, Compston W (1974) 87Sr/86r composition of seawater during the Phanerozoic. Geochim Cosmochim Acta 33:1461–1484

Vejre H, Hoppe C (1998) Distribution of Ca, K, Mg, and P in acid forest soils in plantations of Picea abies—evidence of the base-pump effect. Scand J for Res 13:265–273. https://doi.org/10.1080/02827589809382984

Voerkelius S, Lorenz GD, Rummel S et al (2010) Strontium isotopic signatures of natural mineral waters, the reference to a simple geological map and its potential for authentication of food. Food Chem 118:933–940. https://doi.org/10.1016/j.foodchem.2009.04.125

Wakeel A, Steffens D, Schubert S (2010) Potassium substitution by sodium in sugar beet (Beta vulgaris) nutrition on K-fixing soils. J Plant Nutr Soil Sci 173:127–134. https://doi.org/10.1002/jpln.200900270

Wakeel A, Farooq M, Qadir M, Schubert S (2011) Potassium substitution by sodium in plants. CRC Crit Rev Plant Sci 30:401–413. https://doi.org/10.1080/07352689.2011.587728

Wasson AP, Richards RA, Chatrath R et al (2012) Traits and selection strategies to improve root systems and water uptake in water-limited wheat crops. J Exp Bot 63:3485–3498. https://doi.org/10.1093/jxb/ers111

West JB, Hurley JM, Dudás FÖ, Ehleringer JR (2009) The stable isotope ratios of marijuana. II. strontium isotopes relate to geographic origin. J Forensic Sci 54:1261–1269. https://doi.org/10.1111/j.1556-4029.2009.01171.x

White PJ (2012) Long-distance transport in the xylem and phloem. In Marschner's mineral nutrition of higher plants (pp. 49-70). Academic Press.